LEADING-EDGE BOUNDARY LAYER FLOW

Prandtl's vision, current developments and future perspectives

V. Theofilis[*], A.V. Fedorov[**] and S.S. Collis[***]

[*] *E.T.S.I. Aeronáuticos, U. Politécnica de Madrid, E-28040 Madrid, SPAIN*
(vassilis@torroja.dmt.upm.es)

[**] *Moscow Institute of Physics and Technology, 141700 Moscow Region, RUSSIA*
(fedorov@falt.ru)

[***] *Sandia National Laboratories[†], P.O. Box 5800, Albuquerque, NM 87185-0370, U.S.A*
(sscoll@sandia.gov)

Abstract: The first viscous compressible three-dimensional BiGlobal linear instability analysis of leading-edge boundary layer flow has been performed. Results have been obtained by independent application of asymptotic analysis and numerical solution of the appropriate partial-differential eigenvalue problem. It has been shown that the classification of three-dimensional linear instabilities of the related incompressible flow [**13**] into symmetric and anti-symmetric mode expansions in the chordwise coordinate persists for compressible, subsonic flow-régime at sufficiently large Reynolds numbers.

Key words: Compressible Hiemenz flow, BiGlobal linear instability analysis

1. INTRODUCTION

In the context of external aerodynamics, the flow near the windward stagnation line of a swept cylinder serves as a canonical model of a leading-edge boundary layer. Research into boundary-layer flows over an unswept cylinder immediately followed the discovery of the boundary-layer concept itself. Indeed, it was Prandtl's interest in measuring the pressure on the surface of a cylinder that led to the discovery, by Hiemenz [**4**], of an exact solution of the incompressible Navier-Stokes equations that describes the

[†] Sandia is a multiprogram laboratory operated by Sandia Corporation, a Lockheed Martin Company, for the United States Department of Energy's National Nuclear Security Administration under contract DE-AC04-94AL85000.

stagnation point flow and bears his name. As the performance benefits of swept wings were realized and demonstrated in Göttingen [**5-6**] this solution was extended to the well-known three-dimensional stagnation-line flow [**10**].

Concurrently with the extension of the swept Hiemenz solution to the compressible régime by Reshotko and Beckwith [**9**], investigations into the instability of leading-edge boundary layer commenced. The first instability results were presented 50 years ago with the contributions of Görtler [**1**] and Hämmerlin [**2**] to the meeting "Fifty Years Boundary-Layer Research," celebrating Prandtl's boundary-layer idea. Both those contributions dealt with incompressible *stagnation point* (unswept Hiemenz) flow and put forward what has become known as the Görtler-Hämmerlin (GH) Ansatz, whereby linear disturbances of the leading-edge boundary layer inherit the functional dependence of the basic flow itself. Accordingly, the streamwise and wall-normal disturbance velocity components are functions of the wall-normal coordinate and, in addition, the streamwise velocity component depends linearly on the chordwise spatial coordinate. This Ansatz was later extended [**3**] and verified [**11**] for the incompressible *stagnation line* (swept Hiemenz) flow. These studies demonstrated that the most unstable eigenmode of the leading-edge boundary layer, denoted as the GH-mode, compares well with experiment and direct numerical simulation under linear conditions.

Recent advances in computing hardware and algorithms have permitted generalizations of the GH Ansatz in the context of BiGlobal linear theory based on solution of partial-differential eigenvalue problems (EVP). Lin and Malik [**7**] discovered new eigenmodes besides the GH-mode, and Theofilis, Fedorov, Obrist and Dallmann [**13**] demonstrated that the instability of incompressible three-dimensional swept leading-edge boundary-layer flow is amenable to analysis. The latter authors identified all (BiGlobal) eigenmodes as having a polynomial structure along the chordwise direction and reduced the partial-differential EVP to a system of one-dimensional ordinary-differential EVPs of the Orr-Sommerfeld class. The solution of this system delivers the *complete three-dimensional instability characteristics* for incompressible swept leading-edge boundary-layer flow.

The present contribution demonstrates that this reduction is also possible for compressible flows, albeit restricted to certain ranges of Reynolds and Mach numbers. We proceed along lines analogous to [**13**] and arrive at the instability characteristics of viscous compressible three-dimensional leading-edge boundary-layer flows by independent application of asymptotic analysis [**13**] and a novel numerical solution of the compressible BiGlobal EVP [**14**]. In Section 2 the fundamentals of our theoretical approach are discussed. Section 3 presents details of the basic flow followed by instability

analysis results obtained using both theoretical approaches. A brief discussion of our ongoing efforts closes our present contribution.

2. THEORY

2.1 The basic state

The leading-edge flow in the vicinity of the attachment line of a swept wing is treated as a compressible stagnation line flow, with a non-zero velocity component along the attachment line. If the viscous boundary layer thickness is small compared with the leading-edge radius then the surface near the attachment line can be approximated as locally flat. Under these conditions, the Reynolds number is defined as

$$R = W_e^* \Delta^* / \nu_e^*, \qquad \Delta^* = \sqrt{\nu_e^* / (\partial U_e^* / \partial x^*)_{x=0}} \tag{1}$$

where W_e^* is the spanwise component of the velocity vector (U_e^*, W_e^*) at the boundary-layer edge — a scale consistent with that adopted in [**12-13**]. In the Cartesian coordinate system $(x, y, z) = (x^*, y^*, z^*) / \Delta^*$ (asterisk denotes dimensional quantities), the basic flow quantities are expressed in the form

x-component velocity: $$U_s^*(x, y, z) = W_e^* x U_0(y) / R \tag{2}$$

y-component velocity: $$V_s^*(x, y, z) = W_e^* V_0(y) / R \tag{3}$$

z-component velocity: $$W_s^*(x, y, z) = W_e^* W_0(y) \tag{4}$$

temperature: $$T_s^*(x, y, z) = T_e^* T_0(y) \tag{5}$$

pressure: $$P_s^*(x, y, z) = \rho_e^* W_e^{*2} \left(\frac{1}{\gamma M^2} - \frac{x^2}{2R^2} \right) \tag{6}$$

density: $$\rho_s^*(x, y, z) = \rho_e^* \rho_0(y) = \rho_e^* / T_0(y) \tag{7}$$

viscosity: $$\mu_s^*(x, y, z) = \mu_e^* \mu(T_0(y)) . \tag{8}$$

The profiles $U_0(y)$, $V_0(y)$, $W_0(y)$ and $T_0(y)$ are solutions of the ordinary-differential-equation system [**9**]

$$\frac{1}{T_0}\left(U_0^2 + V_0 U_0'\right) = 1 + \frac{d\mu}{dT_0} T_0' U_0' + \mu U_0'' \tag{9}$$

$$\frac{1}{T_0} V_0 W_0' = \frac{d\mu}{dT_0} T_0' W_0' + \mu W_0'' \tag{10}$$

$$U_0 - \frac{V_0}{T_0} T_0' + V_0' = 0 \tag{11}$$

$$\frac{d\mu}{dT_0} \frac{1}{\mathrm{Pr}} T_0'^2 + \frac{\mu}{\mathrm{Pr}} T_0'' - \frac{T_0' V_0}{T_0} + (\gamma - 1) M^2 \mu W_0'^2 = 0 \,, \tag{12}$$

subject to the boundary conditions

$$U_0(0) = W_0(0) = 0 \,,\; V_0(0) = -C_q T_w \tag{13}$$
$$U_0(\infty) = W_0(\infty) = T_0(\infty) = 1 \,.$$

In these expressions, C_q is a suction parameter, $T_w = T_0(0)$ is the wall temperature, $T_0'(0) = 0$ on adiabatic walls, and $M = W_e^* / a_e^*$ is the local Mach number.

2.2 Asymptotic analysis

The spatial homogeneity of the basic state along z permits the introduction of the decomposition

$$\boldsymbol{Q}(x,y,z,t) = \boldsymbol{Q}_b(x,y) + \boldsymbol{q}(x,y) \exp [\, i\, (\beta z - \omega t\,) \,] \tag{14}$$

into the governing three-dimensional viscous compressible equations of motion. Here, $\boldsymbol{Q}_b$ is the steady basic state, constructed using equations (2-6) after solving the system (9-13), and $\boldsymbol{q} = (u, v, w, \theta, p)^T$ are the *two-dimensional* amplitude functions of the velocity components, temperature and pressure. In the temporal framework considered here, β is a real wavenumber parameter related with a periodicity length $L_z = 2\pi/\beta$ along the spanwise direction, while the frequency ω is the sought eigenvalue. Additional free parameters are the Reynolds and Mach numbers, R and M, respectively.

The extended disturbance vector-function is specified as $\mathbf{F} \equiv (u, \frac{\partial u}{\partial y}, v, p, \theta, \frac{\partial \theta}{\partial y}, w, \frac{\partial w}{\partial y})^T$. Under the assumption of large Reynolds number R, a small parameter $\varepsilon = R^{-1}$ and slow variables $x_1 = \varepsilon x$, $t_1 = \varepsilon t$ are introduced and the vector function is given by the asymptotic expansion

$$\mathbf{F} = \mathbf{Z}_0(y; x_1, t_1, \beta, \omega) + \varepsilon \mathbf{Z}_1(y; x_1, t_1, \beta, \omega) + \ldots \tag{15}$$

The zero-order term is expressed as $\mathbf{Z}_0 = C(x_1, t_1)\boldsymbol{\xi}(y; x_1)$, where $\boldsymbol{\xi}$ is a solution of the eigenvalue problem

$$\frac{\partial \boldsymbol{\xi}}{\partial y} = \mathbf{A}\boldsymbol{\xi} \tag{16}$$

$$\xi_1 = \xi_3 = \xi_5 = \xi_7 = 0\,, \quad y = 0$$

$$\xi_1 = \xi_3 = \xi_5 = \xi_7 = 0\,, \quad y = \infty$$

which delivers the eigenvalue $\omega = \omega_0(\beta, R)$. Here $\mathbf{A}$ is an 8×8 matrix of the stability problem. For the compressible Hiemenz flow, the eigenvalue ω_0 does not depend on x_1 and the eigenvector has the explicit form $\boldsymbol{\xi} = (x_1\xi_{01}(y), x_1\xi_{02}(y), \xi_{03}(y), \xi_{04}(y), \xi_{05}(y), \xi_{06}(y), \xi_{07}(y))^T$. This fact allows for substantial simplifications of further analysis.

The second-order approximation leads to the inhomogeneous problem

$$\frac{\partial \mathbf{Z}_1}{\partial y} = \mathbf{A}\mathbf{Z}_1 + \mathbf{G}_t \frac{\partial \mathbf{Z}_0}{\partial t_1} + \mathbf{G}_x \frac{\partial \mathbf{Z}_0}{\partial x_1} + \mathbf{G}\mathbf{Z}_0 \tag{17}$$

$$Z_{11} = Z_{13} = Z_{15} = Z_{17} = 0\,, \quad y = 0$$

$$Z_{11} = Z_{13} = Z_{15} = Z_{17} = 0\,, \quad y = \infty$$

where $\mathbf{G}_t = i\partial\mathbf{A}/\partial\omega$, $\mathbf{G}_x = -i\partial\mathbf{A}/\partial\alpha$ with $\mathbf{A}$ being derived for the disturbance: $\exp[i(\alpha x + \beta z - \omega t)]$; the matrix $\mathbf{G}$ includes the basic-flow terms associated with nonparallel effects and higher-order terms of the stability problem of the parallel flow. The problem (17) has a non-trivial solution if the inhomogeneous part is orthogonal to the correspondent solution $\boldsymbol{\zeta}$ of the adjoint problem. This leads to the equation for the amplitude function $C(x_1, t_1)$

$$\left\langle \mathbf{G}_t\boldsymbol{\xi}, \boldsymbol{\zeta} \right\rangle \frac{\partial C}{\partial t_1} + \left\langle \mathbf{G}_x\boldsymbol{\xi}, \boldsymbol{\zeta} \right\rangle \frac{\partial C}{\partial x_1} + C\left[\left\langle \mathbf{G}_x \frac{\partial \boldsymbol{\xi}}{\partial x_1}, \boldsymbol{\zeta} \right\rangle + \left\langle \mathbf{G}\boldsymbol{\xi}, \boldsymbol{\zeta} \right\rangle \right] = 0 \tag{18}$$

where the scalar products are defined as $\left\langle \mathbf{G}\boldsymbol{\xi}, \boldsymbol{\zeta} \right\rangle \equiv \int_0^\infty \left(\sum_{j,k=1}^{8} G_{jk}\xi_k, \zeta_j \right) dy$.

Significantly, (18) can be written in a form with structure similar to the incompressible case [**13**],

$$S_1 \frac{\partial C}{\partial t_1} + S_2 x_1 \frac{\partial C}{\partial x_1} + S_3 = 0\,, \tag{19}$$

where S_1, S_2, S_3 are constants. This equation admits the set of solutions

$$C_n(x_1, t_1) = x_1^n \exp(-i\omega_{1n} t_1)\,, \tag{20}$$

$$\omega_{1n} = -i(nS_2 + S_3)/S_1\,,\ n = 0,1,... \tag{21}$$

which give the modes with

$$\mathbf{F}_n(x,y,z,t) = x_1^n \boldsymbol{\xi}(y) + O(\varepsilon)\,, \tag{22}$$

$$\omega_n = \omega_0 + \varepsilon\omega_{1n} + O(\varepsilon^2)\,. \tag{23}$$

Here $n = 0, 2,...$ corresponds to the symmetric modes S1, S2, …, and $n = 1, 3,...$ corresponds to the antisymmetric modes A1, A2, … The first symmetric mode S1 is equivalent to the GH mode.

In summary, the following algorithm is formulated for the calculation of symmetric and antisymmetric modes: 1) Solve the zero-order problem (16) at $x_1 = 0$, which is simply a 2-D stability problem for the parallel boundary layer with the profiles $W_0(y)$ and $T_0(y)$; 2) Solve the corresponding adjoint problem and calculate the coefficients S_1, S_2, S_3 of (19); 3) Calculate the eigenvalues ω_n and the disturbance vector $\mathbf{F}_n$ using the formulae (21)-(23).

2.3 The BiGlobal EVP

Without resort to the explicit dependence of the disturbance quantities on the chordwise coordinate, as done in (15), the chordwise, *x,* and wall-normal, *y*, directions are resolved in a coupled manner. Linearization and subtraction of the basic-flow related quantities lead to a generalized eigenvalue problem that may be converted into a matrix EVP, amenable to numerical solution, once numerical prescriptions for the differential operators (here spectral collocation) and appropriate boundary conditions are provided. The general form of the viscous compressible three-dimensional BiGlobal eigenvalue problem is

$$\mathsf{L}\,\boldsymbol{q} = \omega\,\mathsf{R}\,\boldsymbol{q}, \tag{24}$$

where the entries of the matrices L and R may be found in [**14**]. By contrast to the latter work, in the open flow system considered here, the boundary conditions are no-slip at the wall, $y = 0$; homogeneous Dirichlet at the free-stream, $y = y_\P$; and linear extrapolation from the interior of the computational domain at the endpoints $x = \pm x_\P$ of the truncated domain along the chordwise direction. The related parameters were taken as $y_\P = 100$ and $x_\P = 25$ in all computations performed here. Finally, the EVP (24) was solved using an Arnoldi iteration for the recovery of the relevant part of the eigenspectrum.

3. RESULTS

3.1 The compressible swept Hiemenz basic flow

The basic flow is considered on an adiabatic wall, $T_0'(0) = 0$, the suction parameter is taken $C_q = 0$ and a perfect gas with specific heat ratio $\gamma = 1.4$ and Prandtl number $Pr = 0.72$ is considered. The viscosity coefficient is calculated using Sutherland´s formula at the local temperature $T_e^* = 300\,\mathrm{K}$. The problem (9-13) has been solved using a shooting method. Table 1 shows the dependence of the shear-stress and the wall-temperature on Mach number. Note that a characteristic overshoot in $U_0(y)$ appears at high Mach numbers [**9**], creating an inflection point in this velocity component. This, in turn, may give rise to inviscid instabilities of the compressible leading-edge flow in addition to those known to exist in the compressible flat-plate boundary-layer [**8**].

Table 1. Dependence of basic flow shear-stresses and wall-temperature on *M*.

M	$U_0'(0)$	$W_0'(0)$	$T_0(0)$
10^{-5}	1.232588	0.570465	1.000000
0.25	1.228483	0.566095	1.010746
0.50	1.216689	0.553511	1.042990
0.75	1.198610	0.534132	1.096741
1.00	1.176141	0.509881	1.172016
1.50	1.125582	0.454480	1.387198
2.00	1.076630	0.399360	1.688629
2.50	1.034609	0.350344	2.076344
3.00	1.000514	0.308888	2.550336

3.2 BiGlobal instability of the compressible Hiemenz flow

Results for the symmetric GH (S1), S2 and anti-symmetric A1, A2 modes are presented at the Reynolds number $R = 800$ and subsonic Mach numbers $M = 0.02, 0.5, 0.9$. The case $M = 0.02$ is in good agreement with the incompressible flow discussed in [**13**]. Distributions of the amplification rate $c_i = \mathrm{Im}(\omega_i/\beta)$ at the two first Mach numbers considered are shown in Figure 1. Full lines correspond to results of the analysis of Section 2.2 while symbols denote results obtained by numerical solution of the BiGlobal EVP discussed in Section 2.3. Good agreement may be seen between the results for the most unstable GH-mode predicted by the two approaches. This

reinforces both methodologies as valid research tools to predict instability characteristics within appropriate parameter ranges. It should be noted here that, unlike the case of [**13**] where an explicit closed-form one-dimensional model could be written for the description of three-dimensional eigenmodes, deriving such a model for the compressible leading-edge boundary-layer flow is of limited usage, due to the error in the second-order asymptotic expansion presented, which scales as

$$O(M^2/R^2)\,. \tag{25}$$

Nevertheless, in the appropriate parameter ranges, the spatial structure of the compressible analogues of the modes GH, A1, S2, A2, … closely resemble those of incompressible flow. A demonstration can be seen in the amplitude functions of the GH mode at M=0.5, R=800, β=0.255 shown in Figure 2, where the linear dependence of $u(x,y)$ on x and the independence of $w(x,y)$ (as well as v, θ and p not shown here) can be clearly seen. While this functional dependence is only asymptotically valid in the analysis of Section 2.2, the numerical solution of the BiGlobal EVP, without *a-priori* imposition of the GH Ansatz, delivers the first demonstration of the form of the most unstable linear eigenmode in compressible leading-edge boundary layer flow at these parameters.

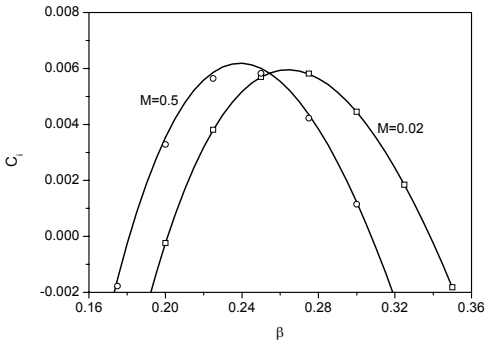

Figure 1. Distributions over β of the amplification-rate c_i of mode GH (S1) at R=800 and M=0.02, 0.5. Solid lines obtained by the asymptotic analysis of Section 2.2, symbols by numerical solution of the BiGlobal eigenvalue problem presented in Section 2.3.

However, as the Mach number increases (keeping all other parameters fixed) the two approaches deviate substantially in their instability predictions. Figure 3 shows that at M=0.9 and R=800 the BiGlobal EVP predicts a slightly wider and substantially stronger amplified flow compared with the asymptotic solution. The agreement improves with increasing Reynolds number, as can be seen in the case of R=1500 shown in the same figure. This is in line with (25), while in both cases Branch I is predicted in

a consistent manner. Work is currently underway to identify the stability boundaries using both approaches.

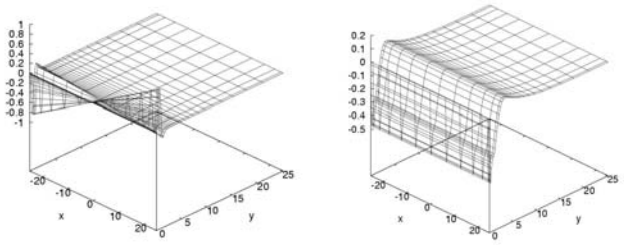

Figure 2. Amplitude functions of the disturbance velocity components of the leading eigenmode at R = 800, β = 0.255, M = 0.5. Left: *u(x,y),* Right: *w(x,y).*

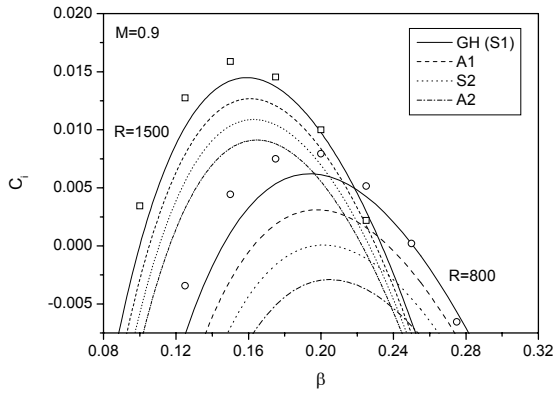

Figure 3. Dependence of c_i on β for modes GH, A1, S2, A2 at M=0.9, R=800 and 1500.

4. DISCUSSION

The first BiGlobal instability analysis of viscous compressible swept Hiemenz flow has been performed. Good agreement between asymptotic analysis and numerical solution of the partial-differential eigenvalue problem has been obtained within appropriate parameter ranges. It has been demonstrated that the three-dimensional "polynomial" eigenmodes of incompressible flow [**13**] persist in the subsonic flow regime. However, differences of the two approaches are found to occur at moderate Reynolds and high Mach numbers. This underlines both the efficiency of the

asymptotic approach at the high-Reynolds number subsonic regime and the need for accurate numerical methodologies in order to provide reliable predictions of instability characteristics of this flow at all speed ranges.

ACKNOWLEDGEMENTS

The work of V. Theofilis was partly supported by the European Office of Aerospace Research and Development, the Air Force Research Laboratory, and the Air Force Office of Scientific Research, under Grant No. FA8655-03-1-3059 monitored by Dr. John D. Schmisseur (AFOSR) and Mr. Wayne Donaldson (EOARD). Additional partial support was provided by a Ramón y Cajal research fellowship of the Spanish Ministry of Science and Technology.

REFERENCES

1. Görtler, H. "Dreidimensionale Instabilität der ebenen Staupunktströmung gegenüber wirbelartigen Störungen". In *50 Jahre Grenzschichtforschung* (ed. H. Görtler, W. Tollmien), Vieweg und Sohn., pp. 304- 314., 1955.
2. Hämmerlin, G. "Zur instabilitätstheorie der ebenen Staupunktströmung". In 50 Jahre Grenzschichtforschung (ed. H. Görtler, W. Tollmien), Vieweg und Sohn, pp. 315-327, 1955.
3. Hall, P, Malik, MR, Poll, DIA. "On the stability of an infinite swept attachment-line boundary layer". *Proc. R. Soc. Lond. A* **395**, pp. 229-245, 1984.
4. Hiemenz, K. "Die Grenzschicht an einem in den gliechförmigen Flüssigkeitsstrom eingetauchten geraden Kreiszylinder. Thesis, Göttingen. Also *Dingl. Polytechn. J.* **326**, pp. 321- 324, 1911.
5. Horten, R., Selinger, P.F. "Nurflügel - Die Geschichte der Horten-Flugzeuge 1933-1960". Weishaupt., 1983.
6. Kármán, T., Edson, L. "The wind and beyond. Theodore von Kármán: Pioneer in aviation and pathfinder in space". Little, Brown & Co. Boston, 1967.
7. Lin, RS, Malik, MR. "On the stability of attachment-line boundary layers. Part 1. the incompressible swept Hiemenz flow". *J. Fluid Mech.* **311**, pp. 239–255, 1996.
8. Mack, LM. "Boundary-layer linear stability theory". *AGARD Rep 709*, 1984.
9. Reshotko, E. and Beckwith, IE. "Compressible laminar boundary layer over a yawed infinite cylinder with heat-transfer and arbitrary Prandtl number". NACA TR1379, 1958.
10. Schlichting, H. "*Grenzschichttheorie",* Braun, 1951.
11. Spalart, PR. "Direct numerical study of leading-edge contamination". AGARD CP-438, pp. 5-1 - 5-13, 1988.
12. Theofilis, V. "On linear and nonlinear instability of the incompressible swept attachment-line boundary layer". *J. Fluid Mech*. **355**, pp. 193-227, 1998.
13. Theofilis, V., Fedorov, A. Obrist, D., Dallmann, UCh. "The extended Görtler–Hämmerlin model for linear instability of three-dimensional incompressible swept attachment-line boundary layer flow". *J. Fluid Mech*. **487**, pp. 271-313, 2003.
14. Theofilis, V., Colonius, T. "Three-dimensional instabilities of compressible flow over open cavities: direct solution of the BiGlobal eigenvalue problem". AIAA Paper 2004-2544, 2004.